Revista Geográfica de Chile Terra Australis Vol.54
ISSN 0719-9562
pp. 13-25

Ash fallout hazard from Irazú volcano, Costa Rica

Peligro de ceniza del volcán Irazú, Costa Rica

Gustavo Barrantes[1], Santiago Núñez[2], Eduardo Malavassi[3]

ABSTRACT

The eruptive period between 1963-1965 at Irazú volcano showed that Costa Rica is highly vulnerable to ash fallout. Ash was carried by wind currents to-wards the Great Metropolitan Area (GMA), southwest to the summit, which contains about 60% of the national population. Previous work on hazard assessment for ash fall at Irazú only estimate influence areas without detailing hazard levels based on the observed distribution of events between 1963-1965. These cartographic models are not suited for realistic risk estimation, informed land use planning or proper emergency management. In this paper, we used the computer code NG-TEPHRA for simulating ash fallout from Irazú volcano, assessing the associated volcanic hazard and developing an improved hazard map from ash fall by devising a hazard index that combines the spatial probabilities of relevant scenarios with estimates of deposited ash volumes. Previous simulations result from our group were already calibrated against observed historical and field (geological) data from the 1963-1965 eruptive period and were used for obtaining the final hazard map. Our results represent a contribution for land use planning and emergency management purposes based on the application of computer models and interdisciplinary research towards numerically informed hazard models.

RESUMEN

Durante el periodo eruptivo entre 1963 y 1965, volcán Irazú mostró que Costa Rica es altamente vulnerable a la caída de ceniza. En esta ocasión la ceniza fue transportada por los vientos hacia la Gran Área Metropolitana (GAM), al suroeste del cráter, área que alberga al 60% de la población del país. Previos trabajos en la evaluación de la amenaza por caída de ceniza del Irazú solo estimaron el área de influencia basados en la distribución observada de los eventos entre 1963-1965 sin detallar la amenaza. Estos modelos cartográficos no son adecuados para una estimación realista del peligro, para el ordenamiento territorial o para la atención de emergencias. En este artículo, utilizamos el código de computadora NG-TEPHRA para simular la caída de ceniza del volcán Irazú, evaluando así el peligro volcánico asociado y desarrollando un mapa de amenaza mejorado de la caída de ceniza, mediante la elaboración de un índice de amenaza que combina las probabilidades espaciales de escenarios relevantes con estimaciones de volúmenes de ceniza depositados. Los resultados de simulaciones anteriores de nuestro grupo permitieron calibrar el modelo con los datos históricos y de campo observados (geológicos) del período eruptivo de 1963-1965 que se utilizaron para obtener el mapa de amenaza final. Nuestros resultados representan una contribución para el ordenamiento territorial y la atención de emergencias con base en la aplicación de modelos informáticos y la investigación interdisciplinaria hacia modelos de amenaza informados numéricamente.

Keywords: Ash fallout. Irazú volcano. Volcanic simulation.

Palabras clave: Caída de ceniza. Volcán Irazú. Simulación volcánica.

[1] Universidad Nacional de Costa Rica. Avenida 1 Calle 1, Heredia 86-3000, Costa Rica, email: gbarrantes@una.cr
[2] Illinois Informatics Institute. University of Illinois at Urbana-Champaign. NCSA Building, 1205 West Clark, Urbana, IL 61801, USA. email: nunezco2@illinois.edu
[3] Universidad Nacional de Costa Rica. Avenida 1 Calle 1, Heredia 86-3000, Costa Rica, email: emalavassi@gmail.com

Fecha de recepción: 7 de marzo 2018
Fecha de aceptación: 31 octubre 2018

INTRODUCTION

Irazú volcano in Costa Rica showed its destructive potential during the eruptive period between 1963 and 1965, affecting severely an estimated area of 100 km2 including the cities of Coronado, Montes de Oca, Curridabat, Llano Grande, San Juan de Concepción, Dulce Nombre, Potrero Cerrado and partially both Desamparados and Goicoechea. A second, larger and less directly affected area (approx. 300 km2) had total estimate losses amounting to $2.000.000,00 USD at the time (Escuela Centroamericana de Geología, 1993). Main damages included crop loss (coffee, potato, corn, tomato), livestock health issues in milk farms and other problems in cities close to the volcano. San José (the capital city, 30 km from the vent) was called at the time the city of brooms (Armbrister, 1964), related to the fact that daily ash fallout deposits were of at least of 1 gm/cm2 during the most intensive episodes. Ash accumulation on the soil lead to debris flows which took the lives of 20 people and destroyed around 300 houses (Waldron, 1967). In 1963, the Costa Rican population reached approximately 1.4 million inhabitants, while current national statistics place the number above 4.3 million (INEC, 2015). The largest affected area included the Great Metropolitan Area (GMA), having the highest urban density with more than 60% of the national population and an approximate 75% of all productive activities in the country (Astorga, 2008).

Hazard assessments for ash fallout start from historical and tephrostrati-graphic records in order to assess the impact of potential eruptive scenarios by retrospectively understanding past eruptions. They provide, when sufficient samples are available, a distribution of the ash from which the violence and energy of the eruption can be inferred. Later, by finding values to key parameters from these, development of scenarios of interest becomes possible (in agreement with the theoretical and practical needs at hand), a more comprehensive spatial estimation of vulnerability and impact can be achieved (Blong, 1996).

For the case of Irazú volcano, the analysis of ash-fall deposit studies in Barquero (1977), Alvarado (1993) and Clark (1993) constitute our baseline evidence for its eruptive processes and potential impact. By combining these with relevant wind profiles (Alvarado and Fernández, 2001; Zárate, 1988), the construction of simulation scenarios becomes possible thanks to the availability of input parameters for applying suitable models. Crisis management and long term urban and rural land use planning are amongst the main purposes of scenario building (Blong, 1996). Our work is a first approximation at estimating volcanic hazard from ash fall at Irazú volcano by means of computer simulations based on the Suzuki ash fallout model, constrained by existing data from which the parameters of the model were estimated. We associated VEI (Newhall and Self, 1982) to each statistically representative scenario in order to establish a classification of eruption episodes; even when VEI does not distinguish between different phenomena within those episodes (Miles et al., 2004), Finally, a hazard index that integrates both spatial probability and ash volume was devised for obtaining a realistic hazard map.

Volcanic hazards from Irazú

Irazú is an active volcano located near the southern end of the Costa Rican section of the Central American Volcanic Arc (CAVA) (Fig 1). The volcanic edifice has a volume of 227 km3 and a height of 3432 m.a.s.l. For the last 2600 years at least Irazú may have erupted around 85 times, where ten of these were large strombolian eruptions (i.e. characterized by VEI = 3) probably every 200– 400 years and the rest are smaller eruptions with VEI 2. Historic eruptive phases have, on average, occurred every 26 yr and continued for periods of hours to more than 3 years (Siebert et al., 2011). Quiescent periods have lasted from less than a year up to 162 yr between the 1561 and 1723 eruptions. We note that it is quite possible that small, VEI = 1 eruptions may have occurred between 1561 and 1723, but were not noted in historical accounts (Clark et al., 2006). The latter is essential in attempting to model the dynamics of many small events and few large ones with the same stratigraphy (Pyle, 1989).

At Irazú, each main eruptive cycle starts with a relatively dry event (Hawaiian-like or Strombolian eruptions) that produces coarse, juvenile, ballistic-like pyroclastic deposits. Later in the eruption, wet explosions (phreatic and phreatomagmatic) occur, generating both wet and dry surge and fallout deposits. Because no systematic chemical difference exists between the deposits from Strombolian and phreatomagmatic eruptions, it can be concluded the main control on the eruptive style of Irazú is the magmatic gas content and the interaction between magma and water, driven as well by magma ascent velocity. The chemical composition of magmas erupted by Irazú during the last 26 centuries is consistent with the latter and corresponds to basaltic and basaltic-andesite magmas and has remained constant (Alvarado et al., 2006).

Ash accumulation is thickest SW off the crater, near the headwaters of the Reventado River in correspondence with the small events, but larger eruption intensities correlate with deposition shifts toward WSW where the capital city, San José is located (Clark et al., 2006). Bombs and blocks reached a distance up to 4 km from the active vent (Paniagua and Soto, 1987).

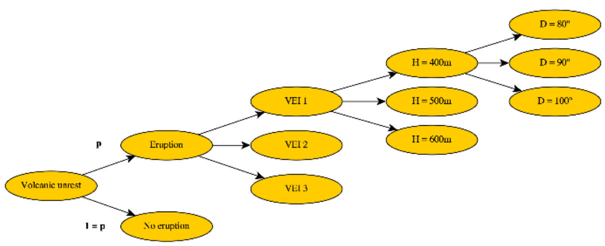

Figure 1: Geographical situation of Irazú volcano in Costa Rica. Nearby volcanic structures are indicated in relation to San José, the capital city.

Cervantes is the most recent lava flow complex at Irazú and one of the largest flow fields in Central America, covering 42 km2 and having a volume of 1 km3 (Figs. 2 and 3). Compound lava flows erupted from two of several N-S aligned vents on the southeastern slope of Irazú volcano (Thomas, 1983; Tournon, 1984; Clark et al., 1998; Alvarado et al., 2006; Benjamin et al., 2007). The Cervantes lava fields have been dated at 14500 ±160 years (Sáenz et al., 1982). Additionally, during the climax of the 1963-1965 eruption in December, 1964 a lava pool formed at the bottom of the active vent for several days, but no more lava flows were issued (Murata et al., 1965).

Other hazards at Irazú include lahars that descended from the volcanic edifice along the principal drainages (Reventado, Sucio, Toro Amarillo and Birris) during active periods. These are product of a combination of factors: (1) the presence of abundant volcanic ash on the ground that deteriorates the vegetable coverage and develops a superficial crust on the ash deposits, more impermeable than the ground surface; (2) the high pluviosity over the volcanic edifice; (3) the steepness of slopes and the instability of the flanks (Waldron, 1967) partially induced by several active faults around the volcanic edifice (Barboza et al., 2001). Also, partial collapses are induced by hydrothermal alteration of the flanks as well as slope instability (Krushensky, 1972).

Simulation of the ash fallout process

During the past 30 years modeling and simulation of volcanic processes have become more relevant to understanding ash fallout. Recent advances on high performance computing have increased the accuracy of computer simulation in the geophysical sciences. Good agreement between computed and observed data justifies their applications to real-case scenarios (Bonadonna, 2006).

Numerical modeling and probability estimation for different classes of eruptions have contributed largely during the last decade to a better understanding of plume dynamics. Geological records are typically biased towards the largest events that have been recorded deposits left by small eruptions are often re-moved by erosion (Connor et al., 2001). On the other hand, the product of wind profiles and severity of the eruptions (as estimated by the VEI) is a necessary element in the realistic determination of hazard by ash fallout.

The use of ash fallout models depends on both the modeling objective and the availability, amount and quality of the experimental observations. Most models fall within the Eulerian (continuous) or Lagrangian (particle tracking) categories, for which 2D and 3D domains are used (Scollo et al., 2008). 3D models imply higher CPU cost and better observational data, being impractical for most computing infrastructure in the developing countries, in particular for real-time modeling. On the other hand, some 2D models simplify or remove elements such as topography or wind profiles, critical for accurate estimations. A compromise between computational cost and accuracy was preferred in this case, therefore using a semi-empirical model (instead of departing from either strict ab initio or stochastic approaches), with the advantage of having analytic equations that describe ash accumulation and are easy to compute.

In this research, hazard assessment of ash fallout at Irazú volcano was obtained by using a new implementation of TEPHRA code, namely NG-TEPHRA, and the development of a methodology that estimates hazard by formulating an index based on ash accumulation and its probability from statistically representative scenarios.

The advection-diffusion model.

Models of ash sedimentation from volcanic plumes are devised from a mass-conservation equation. Most of them describe tephra dispersion as an advection process where particles leaving the plume exhibit vertical, linear diffusion above the eruptive vent (Bonadonna, 2006). Additional simplifications include taking tephra terminal velocity as constant (depending on particle size), constant and isotropic horizontal diffusion coefficients and considering vertical diffusion and vertical wind velocity as negligible (Suzuki, 1983). Details of the underlying formulation can be found in Armienti et al. (1988).

TEPHRA is an implementation of the Suzuki model (Suzuki, 1983) designed to calculate ash accumulation in UTM grid coordinates. Its formulation in terms of numerical methods and the corresponding computational implementation are detailed in Connor et al. (2001), and was mostly targeted at execution on Beowulf clusters. A complete description of the code is reviewed in Connor (2002). It has been successfully applied both in forecasting (Scollo et al., 2009) and hazard assessment (Bonadonna et al., 2005) of ash fallout.

The code used in this research is a version of TEPHRA modified for fast execution in individual processors, Beowulf clusters and highly distributed cloud computing architectures (NG-TEPHRA). NG-TEPHRA maintained the formulation of the Suzuki model in TEPHRA, but improved aspects of efficiency and numerical accuracy in order to run in single computing instances within memory limits as to avoid using swap space or any other form of storage. Additional tools were implemented in order to facilitate data gathering and overall statistical analysis. The code allows the execution of massive cloud experiments where one instance of the program represents one scenario, all scenarios execute concurrently, and the individual parameters in each scenario determine if it is allowed to run or is discarded depending on the results of applying a restriction logic, derived from geological principles in the parameter sweep engine (NIMROD). Further details on the computational setting, the design of the experiments and numerical results can be found in Núñez et al. (2010).

Considering that our choice of TEPHRA versus TEPHRA2 (Bonadonna et al., 2005) implies strong simplifications, it is rooted in two main reasons: (1) this exercise is a first approximation where topographic aspects were simplified and (2) wind profile information with sufficient accuracy for interpolation to be meaningful is not available.

Probability-based hazard maps.

Classical geological studies based on the stratigraphic record are insufficient for a complete reconstruction of volcanic hazard and later risk mitigation Bonadonna (2006). Tephra deposits are not necessary preserved on the stratigraphic record when the set wind profiles relevant to the VEI is incomplete. (Bonadonna, 2006) proposed several ways to construct a probabilistic analysis of tephra dispersions, where probability maps and hazard curves based on return periods prove valuable for risk management. They are however difficult to implement because reliable data about the frequency distribution of eruptions must exist. This research focuses on probability maps thanks to the availability of tephra-chronological studies and historical records for Irazú volcano.

The average of past eruptions frequency is assumed to represent the frequency of future eruptions. The annual frequency of a particular eruption is given by

$$\mathrm{P} = \mathrm{N}/\mathrm{T}$$

where P is the annual probability of a particular eruption and N is the total number of eruptions from that volcano in a period of interest (T). Thus, the recurrence interval Tr in years for a particular eruption becomes

$$\mathrm{Tr} = 1/\mathrm{P}$$

The percent-scaled probability and the recurrence interval are related by the formula

$$100 * \mathrm{P} = \frac{100}{\mathrm{Tr}}$$

In order to obtain a reliable statistical assessment of eruptions, a probabilistic event tree was constructed for each VEI following the work of Jenkins et al. (2012). The estimation of the spatial likelihood of each scenario requires knowledge of the most frequent (i.e. likely) wind directions. Each scenario for which a probability can be assigned is then simulated with NG-TEPHRA. Finally, the result map can be visualized using a standard geographic information system (GIS).

MATERIALS AND METHODS

Our approach combines tools and procedures proposed by Connor et al. (2001), Bonadonna (2006), Jenkins et al. (2012) and INETER (2005). An index of ash fall hazard was obtained in four steps: 1) calculation of a probability assessment tree for all scenarios, 2) calibration of the computational model with known events for Irazú volcano, 3) definition and execution of all scenarios, and 4) development of an ash fallout hazard map for later evaluation and analysis by domain experts.

Calculation of a probability assessment tree.

The root node (level zero) represents the total probability of all scenarios. The first level accounts for the probability of an eruption based on historical accounts and tephrachronological data (Fig. 2). The second level estimates the relative probability of VEI values being equal to 1, 2, 3 or higher according to Eqs. 5–7, the historical accounts and geological records provided by Barquero (1977), Murata et al. (1965), Clark (1993) and Escuela Centroamericana de Geología (1993). The third level estimates the probability of a given column height according to ranges established in Newhall and Self (1982) with respect to VEI using a Weibull probability density function in agreement with existing data for the eruptive episode between 1963–1965 (Murata et al., 1965; Barquero, 1977). Finally, the fourth level of the tree is given by the relative frequency of average wind directions for each column height based in local meteorological data (Alvarado and Fernández, 2001) (Fig. 2). The conditional probability of a particular scenario (leaf node) is equal to the product of the probabilities (vertices) starting from the root node to it.

Calibration of the computational model.

Tephra density, form factor and size were obtained from technical reports dating from the eruptive period and subsequent research (Murata et al., 1965; Barquero, 1977; Alvarado, 1993). These parameters were adjusted after calibrating the Suzuki model (Barrantes and Núñez, 2012) using a semi-qualitative approach. A fully quantitative approach was not possible due to the limited extent of directly available data from the

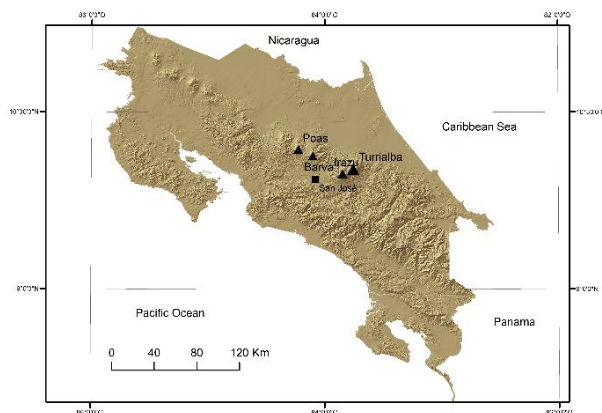

Figure 2: Schema of the probability assessment tree. The state of volcanic unrest, given in practice by the value of precursors, establishes the probability of affectation for a given location by a volcanic eruption (P (x; y)), spatially determined by the volcanic explosivity index (VEI), the height of the ash column (H) and wind direction (D).

emergency period (dating from 1963-1965 or previously) or from later field studies due to weather-driven erosion. The calibration set contains data from eruptions in 1963 during March (22, 23), April (17, 20, 23 and 25), October (23) and December (1). A complete description of the calibration process is described in Barrantes et al. (2013).

A potential caveat is that the Suzuki model has not often been used to model violent eruptions. However, in the case of Irazú Volcano, after the onset event (violent) the remaining events were characterized by passive ash emission, despite of them being Strombolian. A possible geophysical mechanism is the preliminary opening of conducts by a violent event, followed by steady-state magma ascent. Therefore, although the first event may not conform to the Suzuki model, the vast majority of the others will.

Definition and execution of simulation scenarios.

The final probability assessment tree contains 51 scenarios representing potential eruptions that were either observed or likely for the period 1963-1965 according to available historical records: 23 at VEI 1, 17 at VEI 2, and 11 at VEI 3. For each VEI, wind directions were determined using daily reports of upper winds from the weather station at the Juan Santamaría International Airport (SJO), constrained by radiosonde information. Details for each scenario are contained in Table 1.

The probability of each scenario was set a priori according the procedure described above. The estimate of erupted mass for a given column height (H) per unit area in gm/cm2 (M) was obtained from the power law (Bonadonna, 2006).

$$\mathrm{M} = \rho \left(\frac{H}{1670}\right)^{4} \tau$$

While this estimate is conservative and somewhat general, it provides a good starting point. Numerical calculations were performed using the instance of NG-TEPHRA installed on the computing cluster at Universidad Nacional, Heredia, Costa Rica. Output files were imported on the ArcMap SIG for cartographic processing and visualization.

Table 1: Selected simulation scenarios. Columns: ID (scenario), VEI (volcanic explosively index), H (column height in meters), D (wind direction in degrees) and associated probabilities.

ID	VEI	H	D	PV EI	P_H	PID
1	1	400	80	0.569	0.271	0.039
2	1	400	90	0.569	0.271	0.065
3	1	400	100	0.569	0.271	0.039
4	1	500	90	0.569	0.126	0.012
5	1	500	100	0.569	0.126	0.03
6	1	500	110	0.569	0.126	0.012
7	1	500	120	0.569	0.126	0.012
8	1	600	90	0.569	0.139	0.014
9	1	600	100	0.569	0.139	0.033
10	1	600	110	0.569	0.139	0.014
11	1	600	120	0.569	0.139	0.014
12	1	700	90	0.569	0.149	0.014

Continue Table 1: Selected simulation scenarios. Columns: ID (scenario), VEI (volcanic explosively index), H (column height in meters), D (wind direction in degrees) and associated probabilities.

ID	VEI	H	D	PV EI	P_H	PID
13	1	700	100	0.569	0.149	0.036
14	1	700	110	0.569	0.149	0.014
15	1	700	120	0.569	0.149	0.014
16	1	800	90	0.569	0.156	0.015
17	1	800	100	0.569	0.156	0.037
18	1	800	110	0.569	0.156	0.015
19	1	800	120	0.569	0.156	0.015
20	1	900	90	0.569	0.16	0.015
21	1	900	100	0.569	0.16	0.038
22	1	900	110	0.569	0.16	0.015
23	1	900	120	0.569	0.16	0.015
24	1	1000	90	0.05	0.16	0.005
25	1	1000	100	0.05	0.16	0.012
26	1	1000	110	0.05	0.16	0.005
27	1	1000	120	0.05	0.16	0.005
28	2	2000	80	0.345	0.45	0.026
29	2	2000	90	0.345	0.45	0.065
30	2	2000	110	0.345	0.45	0.026
31	2	3000	80	0.345	0.283	0.017
32	2	3000	90	0.345	0.283	0.032
33	2	3000	110	0.345	0.283	0.032
34	2	4000	80	0.345	0.15	0.009
35	2	4000	90	0.345	0.15	0.017
36	2	4000	110	0.345	0.15	0.017
37	2	5000	70	0.345	0.07	0.002
38	2	5000	80	0.345	0.07	0.006
39	2	5000	90	0.345	0.07	0.004
40	2	5000	230	0.345	0.07	0.002

41	3	6000	70	0.086	0.617	0.004
42	3	6000	80	0.086	0.617	0.013
43	3	6000	90	0.086	0.617	0.009
44	3	6000	230	0.086	0.617	0.004
45	3	7000	70	0.086	0.269	0.006
46	3	7000	80	0.086	0.269	0.004
47	3	7000	230	0.086	0.269	0.006
48	3	8000	50	0.086	0.617	0.002

Conclusion Table 1: Selected simulation scenarios. Columns: ID (scenario), VEI (volcanic explosively index), H (column height in meters), D (wind direction in degrees) and associated probabilities.

ID	VEI	H	D	PV EI	P_H	PID
49	3	8000	60	0.086	0.617	0.002
50	3	8000	230	0.086	0.617	0.003
51	3	8000	240	0.086	0.617	0.002

Development of the hazard map

For each location (x, y), M and P were used in order to assess whether a potential damage threshold was reached (Bonadonna, 2006). M (x; y) ≤ 0.25 gm/cm2, P (x, y) ≤ 0.1 were set as a minimum threshold due to potential impact to the Central Valley, an urban area where small amounts of volcanic ash can affect human health, crops, electrical machinery and high-tech facilities that use dust filters. After thresholding, the mass value was replaced by the probability P (x, y) of each specific scenario s. The accumulated probability Pa (x, y) for each location was then calculated as $\sum_s Ps(x, y)$. Fourth and finally, Pa (x, y)'s for all locations were clustered into five probability classes. A similar process was carried out for quantification of accumulated mass. For all locations where M (x, y) exceeded the threshold, Ma (x, y) = $\sum_s Ms(x, y)$ was obtained. Ma (x, y)'s for all locations were similarly clustered into five classes. Finally, both classifications were combined into a discrete ash fallout threat index (Table 2). The index τ [Ma(x, y); Pa(x, y)] is calculated as $\tau[Ma\,(x, y), Pa\,(x, y)] = I\,[Ma(x, y)\,] * I\,[Pa(x, y)]$

where

$$I[\mathrm{Ma(x;\ y)}] = \begin{cases} 1 & \mathrm{Ma(x;\ y)} > 75 \\ 2 & 25 < Ma((x, y \leq 75) \\ 3 & 5 < Ma((x, y \leq 25)6) \\ 4 & 0.25 < Ma((x, y \leq 5) \\ 5 & Ma((x, y \leq 0.25) \end{cases}$$

$$I[\mathrm{P\,a(x;\ y)}] = \begin{cases} 1 & \mathrm{Ma(x;\ y)} > 0.5 \\ 2 & 0.35 < Ma((x, y \leq 0.5) \\ 3 & 0.25 < Ma((x, y \leq 0.35) \\ 4 & 0.10 < Ma((x, y \leq 0.25) \\ 5 & Ma((x, y \leq 0.10) \end{cases}$$

The individual threat levels are defined as follows: extremely high, τϵ {1,2,3}; very high, τϵ {4,5,6}; 6g; high, τϵ {7,8,9}; moderate, τϵ {12,15}; low, τϵ {16,20}; 20g; very low, $\tau\epsilon$ {25}.

RESULTS

All output data sets were converted to maps using a geographic information system (GIS). Two results were obtained after summarizing: a map of accumulated probability (Fig. 3A) and another one for accumulated mass (Fig. 3B). Fig. 3A shows that the probability of accumulation ash is greater on the western flank of Irazú volcano, since the most frequent wind directions run west, followed in frequency by west-northwest and west-southwest directions. On the other hand, in Fig. 3B the distribution of accumulated mass aligns toward the southwest and northeast because large eruptions (VEI 2) balance the effect of the more frequent, smaller eruptions. The latter is due to eruptions reaching altitudes beyond 7000 m.a.s.l., where the principal winds change their direction from southwest to northeast.

Table 2: Coding for the discrete ash fallout threat index. Ma is given in gm/cm2. Color legend: extremely high, very high, high, moderate, low, very low.

	P a	> 0.5	0.5–0.35	0.35–0.25	0.25–0.10	< 0.10
Ma	I(Ma)=I(P a)	1	2	3	4	5
> 75	1	1	2	3	4	5
25–75	2	2	4	6	8	10

5–25	3	3	6	9	12	15
0.25–5	4	4	8	12	16	20
< 0.25	5	5	10	15	20	25

A hazard map was produced using the discrete ash fall threat index by combining the accumulated probability map and the accumulated mass map. Each value for both M a(x; y) and P a(x; y) was classified according to the discrete ash fall threat index and colored as indicated for each hazard level (Table 2). The joint effect of frequent, small eruptions and infrequent large ones leads to a two-lobed distribution with higher hazard intensity towards the GMA, but with a significant lobe towards the northeast from the vent. The interpretation of the map is as follows: the frequency of small eruptions (VEI=1, VEI=2) and ash transport in the southwest wind direction account for most of the accumulated mass, as well as some of the large eruptions where the wind direction is the same. When wind direction changes to the northeast direction depending on the time of the year, large eruptions (VEI=3) contribute to a noticeable northeast accumulation. The latter is consistent with historical accounts of ash deposits in some locations of the Limón province reported in Barquero (1977). The spatial distribution of mass accumulation by ash fallout is dependent upon two main factors: VEI and wind direction (Fig. 4).

The area with the highest threat index is located near the summit, west-northwest of the volcanic structure, close to the headwaters of the Sucio, Blanco and Reventado rivers. This is relevant in particular for the national telecommunications infrastructure: antenna towers of the major television networks and the national incumbent operator are located directly at summit of Irazú volcano. Additionally, lahars have been reported at the headwater of the Reventado river in several occasions (90 lahars were reported only in 1964). The lahar between December 9 and 10, 1963 destroyed 300 houses and caused 20 human casualties (Waldron, 1967). The area marked as of extremely high threat is not limited to Irazú volcano National Park, but extends west-southwest to the Cabeza de Vaca and Retes hills where ash accumulation and the subsequent probability of lahars are also highest. The anastomosing pattern in geomorphology of the region northwest of the vent is indicative of transport and accumulation of sediments that ultimately transit the alluvial fan of the Sucio river, suggestive of large deposits of ash flowing downstream during long periods. Due to the inability to register wind deflation, our results are not able to account for greater ash

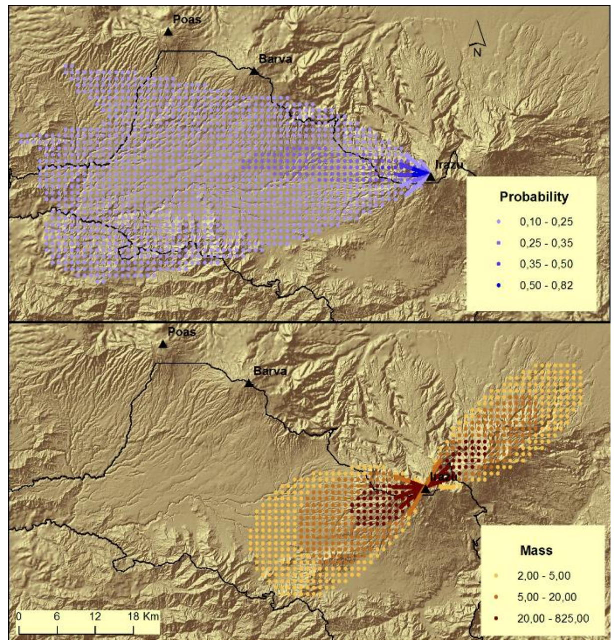

Figure 3: Accumulated ash fallout probability (A) and mass (B). While the latter exhibits a two-lobe distribution due to large eruptions and northeast winds, the probability concentrates west-southwest and west of the vent. Wind northwest directions have a very low probability of occurrence.

accumulations towards the Reventado river as reported in Clark et al. (2006). The area of very high threat has an approximate diameter of 1 km, elongated towards west and northeast of the summit. Mostly cattle ranches with sparse housing are found in it, including scarce transportation infrastructure which might be severely impacted, therefore making evacuation and emergency management more difficult. The high threat area is located both to the south-west and the northeast of the summit, with land use composed mostly of cattle ranches and extensive crops, including some small towns such as Rancho Redondo and Llano Grande at the west-southwest, and sparse towns near Turrialba Volcano at the northeast. The moderate threat area follows the same contour, but in this case includes dense residential areas, such as San Isidro de Coronado and Tres Ríos, southwest of the crater. The low threat area corresponds to the largest urban area of the country, the GMA which includes San José, the capital city, Desamparados and Hatillo (high density residential areas) and the Juan Santamaria (SJO) International Airport.

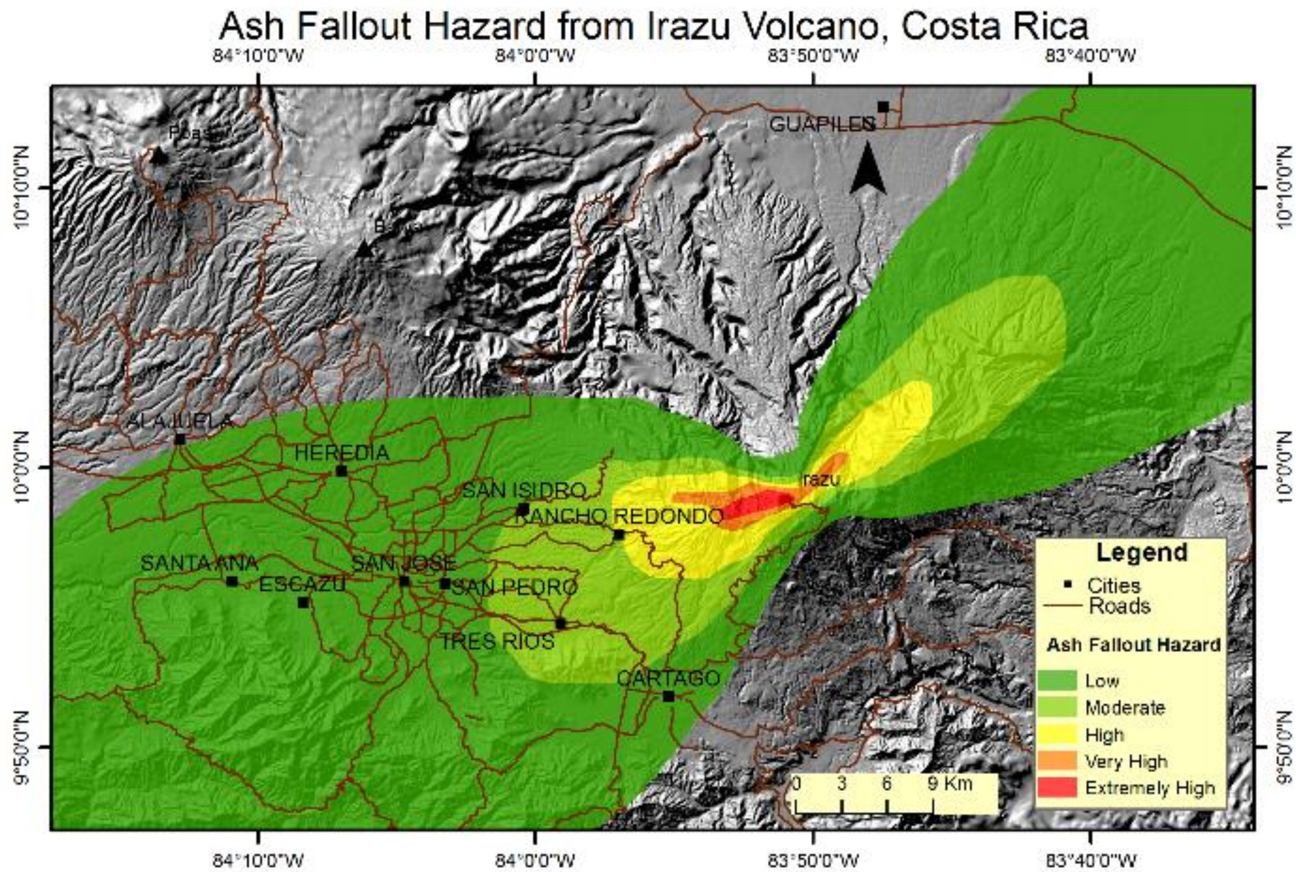

Figure 4: Hazard map obtained from calculating I[Ma(x; y;); P a(x; y)]. Coloring is given according to Table 2. Ash fallout distribution is characterized by two lobes in the west-southwest and northeast directions respectively. The most relevant cities in the GMA are indicated as well

DISCUSSION

Our work represents a significant advancement with respect to existing ash fallout hazard assessments for the Irazú volcano. Previous efforts focused on (a) either showing the final ash distribution during the 1963-1965 eruptive period (Barquero, 1977; Alvarado, 1993; Clark, 1993), (b) performing general evaluations of hazard based on observational methods at a regional scale (Soto and Paniagua, 1992) or (c) performing hazard assessments for the worst possible scenario (Escuela Centroamericana de Geología, 1993). We are able for the first time to properly account for the effect of both small frequent eruptions and large infrequent ones in a semi-quantitative way that bears closer resemblance to historical records and field data than in previous exercises. In particular, the pseudo-isopach map presented by Clark et al. (2006) for deposits dating back from 2600 years as well as the isopachs for the 1963-1965 eruptive period are consistent the observed distribution in our map. The mixed effect of large and small events is clear in the two-lobed distribution of Fig. 4 and is explained by the fact that the probability of an eruption is inversely proportional to its VEI: small eruptions occur more frequently than large ones. However, larger (i.e.

less frequent) eruptions have a stronger impact by releasing significantly larger amounts of ash. In conjunction with total erupted mass, wind direction at high altitudes drives the distribution of ash fallout (Alvarado and Fernández, 2001) in large events.

Simulation-based assessments allowed recreation of events similar to those observed during 1963-1965, and also of those of potential relevance that have not yet occurred or have not been documented properly. The design of simulation scenarios as well as their execution and analysis were possible thanks to the NG-TEPHRA computer application (Núñez et al., 2010) and later post-processing of resulting data using a geographic information system.

Scollo et al. (2008) present a comparative evaluation of three computer codes –namely TEPHRA, HAZMAP y FALL3D- with respect to scenario accuracy by comparing simulation outputs with satellite imagery. The latter research concluded that the difference in the accuracy between simple and complex models depends on the uncertainty and number of input variables in the case of complex models, which in turn generate complex errors. Those are similar in magnitude to errors due to abstracting phenomena with fewer variables and making assumptions that result in simpler models. Unless input data are available for careful calibration in sufficient amounts and with good quality, using complex models does not provide any significant advantage to understanding eruptive activity. In Costa Rica, finding sufficient data for complex models has been infeasible. NG-TEPHRA is as a simpler tool whose results can be more easily verified through existing field observations and historical documents. TEPHRA has been successfully applied along with other software applications such as PUFF within a forecast platform for the Etna volcano (Scollo et al., 2009), where TEPHRA as a lower-accuracy model guided PUFF.

An analysis by Zárate (1988) on the influence of meteorological events over ash dispersion during volcanic eruptions in Costa Rica indicates that transport of materials during the dry season would happen towards the west and the southwest of the vent. The latter is due to trade winds between 1500 y 2500 m.a.s.l. Moreover, when ash columns reach the upper troposphere, the direction of transport is shifted northeast and east of the vent; in the rainy season the direction becomes southwest and northeast. Those directions are in agreement with the results of our simulations using data from Alvarado and Fernández (2001) and others, except for those at the east and northeast. That disagreement might be due to our use of a larger data set (monthly aggregate data) than that of each reference study where east and northeast directions are included and considered as of low probability (Fig. 4). In consequence, only a single eruptive episode is reported for each direction across the whole 1963-1965 eruptive period (Barquero, 1977). A detailed look at the simulation results suggests that the dispersion axes of the ash fallout is consistently oriented west-southwest as noted before in Clark et al. (2006).

The resulting hazard map provides improved guidance for prevention and mitigation actions by indicating areas more prone to being affected by ash fall-out. It allows identification of settlements susceptible to large volumes of ash fallout during volcanic eruptions and later develop proper evacuation plans that promote the organization of communities towards facing eventual emergencies. On the other hand, improved versions of the map are a valuable resource for land use planning by indicating the degree of hazard associated to a region in a discrete scale. For instance, the authors do not recommend future residential, agricultural or industrial development projects in areas of extremely high or very high threat. Both types of areas should be completely incorporated into the limits of Irazú volcano National Park in order to avoid human or material losses. With respect areas rated as of high threat, land usage for farming and low density housing should be preferred. For areas rated as of moderate threat, low density to medium density housing developments is suggested along with enforcement of the construction code requiring roofs with a slope over 30° , thus preventing ash accumulation. Finally, areas rated as of low threat should plan for the potential effects of ash fallout during a large eruption in terms of communications, air traffic and transportation networks, sewage systems and health attention in main cities, with a special focus in the effects derived from small ash particles that travel long distances.

CONCLUSIONS

Modeling and simulation are valuable techniques for obtaining knowledge of past volcanic events, provided that sufficient calibration data exist. The quality of the final threat –and later hazard-estimation depends on reliable observations and, with large recurrence periods for volcanic events, a risk of losing relevant evidence or of its degradation increases with the difference between the most recent eruption and the time at which field samples are collected for small eruptions. Scarcity of data has been the main challenge during our current work, and overcoming data limitations has proven to be a hard issue.

Despite the inherent limitations of semi-empirical models (such as Suzuki's), the results already obtained for Irazú volcano are more detailed than the current cartographic model for hazard assessment; they also appear to be a better match for the distribution of tephra deposits in the recent geological and historical past. By using a simpler model and sensible data, obtaining reasonable results was computationally efficient (in the order of minutes for an approximate area of 4600 km2 and an average distance of 1 km between grid locations) without resorting to more complex mathematical formalisms with input parameters that were unavailable. Building on this research effort, the development of a more comprehensive model that extends NG-TEPHRA is required, but the main trends in tephra distribution will most probably be similar. An improved model will provide a refined view both in terms of geographical accuracy and numerical stability as long as more and better data becomes available.

In the experience described herein, the research process has gone through a series of steps from general, large-scale simulations (4,410,000 scenarios) to geophysical-restricted simulations (98,000 scenarios) to scenario-specific simulations (51 scenarios). Gaining sufficient knowledge for drawing conclusions has required close involvement with the computational component of the research, in particular for developing appropriate techniques for treating large volumes of data and designing heuristics that evaluate the statistical relevance of scenarios before their execution. Although the results presented here are promising for realistically describing scenarios belonging to the 1963-1965 eruptive period for Irazú volcano, more work is required to assess hazard in future eruptions through the incorporation of a detailed quantification of assets in the potentially affected areas.

ACKNOWLEDGEMENTS

The authors wish to acknowledge support of the Direction of Information and Communication Technologies at Universidad Nacional in Costa Rica and the Computer Research Center at the Instituto Tecnológico de Costa Rica for continuous support with the computer cluster during this research, as well as the MeSsAGE Lab at Monash University in Australia and Dr. David Abramson at the University of Queensland in Australia. The authors also wish to thank the multi-year support of the Pacific Rim Applications and Grid Middleware Assembly (PRAGMA) for providing computational resources and expertise in the e-Science component of this work. This process would not have been possible without the financial assistance of the Systems Fund for High Research of the National Council of Rectors (CONARE) in Costa Rica.

REFERENCES

Alvarado G.. Volcanolgy and petrology of Irazú Volcano, Costa Rica. PhD thesis, University Christian-Albrechts, Kiel, 1993.

Alvarado G. E., Carr M. J., Turrin B. D., Swisher C. C., Schmincke H.-U., and Hudnut K. W.. Recent volcanic history of irazú volcano, costa rica: Alternation and mixing of two magma batches, and pervasive mixing. Geological Society of America Special Papers, 412. 2006. Page 259–276,.

Alvarado L. F. and Fernández W.. Climatología de la atmósfera libre sobre Costa Rica. Topicos Meteorologicos y Oceanograficos, 8(2). 2001.Pages 89–115,.

Astorga, A. Análisis de Alcance Ambiental del Plan GAM; Parte II. Technical report, PRUGAM, San José, Costa Rica, 2008.

Armbrister T.. The sky is falling. Saturday Evening Post, 237(20), 1964.

Siebert L., Simkin T., and P. Kimberly. Volcanoes of the World. Univ. of California Press, 2011.

Armienti P., Macedonio G., and Pareschi M. T.. A numerical model for sim-ulation of tephra transport and deposition: Applications to may 18, 1980, mount st. helens eruption. Journal of Geophysical Research: Solid Earth, 93 (B6).1988. Pages 6463–6476,.

Barboza V., Brenes J., Vega F., Malavassi E., González V., and Segura J.. Memoria del congreso nacional de investigación 2000: Sismicidad tecton-ica en el macizo del irazú. Technical report, Consejo Nacional de Rectores (CONARE), 2001.

Barrantes G. and Núñez S.. Análisis de sensibilidad del modelo tephra – informe interno del proyecto tefra-irazu: Escuela de ciencias geograficas. Technical report, Universidad Nacional de Costa Rica, 2012.

Barrantes G., Núñez S., Castro J., Malavassi E., and Soto C.. Simulación de caída de ceniza del volcán irazú aplicando el programa tephra modificado. 2013. Geo UERJ, 1(24),.

Barquero J.. El volcán Irazú y su actividad. Licenciate's degree thesis, Univer-sidad Nacional de Costa Rica, 1977.

Benjamin E. R., Plank T., Wade J. A., Kelley K. A., Hauri E. H., and Alvarado G. E.. High water contents in basaltic magmas from irazu volcano, costa rica. Journal of Volcanology and Geothermal Research, 168(1). 2007.Page 68–92,.

Blong R. J.. Volcanic Hazards Risk Assessment. In Monitoring and Mitigation of Volcano Hazards, pages 675–698. Springer Berlin-Heidelberg, 1996.

Bonadonna, C., Connor, C. B, Houghton B. F., Connor L., Byrne M., Laing A., and Hincks T. K.. Probabilistic modeling of tephra dispersal: Hazard assess-ment of a multiphase rhyolitic eruption at tarawera, new zealand. Journal of Geophysical Research: Solid Earth, 110(B3), 2005.

Bonadonna C., Probabilistic modelling of tephra dispersion. In Statistics in Volcanology. Special Publications of IAVCEI, Geological Society, London, 2006. Pages 243–260.

Clark S. K., Reagan M. K., and Trimble D. A.. Tephra deposits for the past 2600 years from irazú volcano, costa rica. Special Paper- Geological Society of America, 412. 2006. Pages 225–234,.

Clark S. K., Reagan M. K., and Plank T.. Trace element and u-series systematics for 1963-1965 tephras from irazu volcano, costa rica: Implications for magma generation processes and transit times. Geochimica et cosmochimica acta, 62 (15): 1998. Pages 2689–2699.

Clark S. K.. The recent eruptive history of Irazú volcano, Costa Rica: a study of tephra deposits of the last 2,500 years with geochemical and isotopic analysis of the 1963-65 eruption. Master's thesis, Iowa University, 1993.

Connor C., Hill B., Winfrey B., Franklin N., and La Femina P.. Estimation of volcanic hazard from tephra fallout. Natural Hazards Review, 2001. Page 33–42.

Connor C.. Tephra dispersion modeling in parallel, 2002. URL www.cas.usf. edu/~cconnor/parallel/tephra/tephra.html,(retrieved onJune10, 2012).

Escuela Centroamericana de Geología. Amenaza y estimación económica básica de la vulnerabilidad material asociada al Volcán Irazú Cordillera Central. CEPREDENAC, San José, 1993.

INEC. Proyeciones y Estimaciones, 2015. URL http://www.inec.go.cr/Web/ Home/GeneradorPagina.aspx.

INETER. Metodologías para el análisis local de amenazas naturales y riesgos en nicaragua, 2005. URL http://web-geofisica.ineter.gob.ni/proyectos/ metalarn/index.html.

Jenkins S., Magill C., McAneney J., and Blong R.. Regional ash fall hazard I a probabilistic assessment methodology. Bulletin of Volcanology, 74(7). 2012. Pages 1699–1712.

Krushensky D.. Geology of the istarú quadrangle, costa rica. Geological Survey Bulletin 1358, 1972. page 46p.

Miles G., Grainger R., Highwood E., et al. The significance of volcanic eruption strength and frequency for climate. 2004. Quarterly Journal of the Royal Meteoro-logical Society, 130(602). Page 2361–2376,.

Murata K. J., Dondoli C., and Sáenz R.. The 1963-65 eruption of irazú volcano, costa rica (the period of march 1963 to october 1964). Technical report, U.S. Geolgical Survey, 1965.

Newhall C. G. and Self S. The volcanic explosivity index (vei) an estimate of ex-plosive magnitude for historical volcanism. Journal of Geophysical Research: Oceans, 87(C2). 1982. Page 1231–1238,.

Núñez S., Bethwaite B., Brenes J., Barrantes G., Castro J., Malavassi E., and Abramson D.. Ng-tephra: A massively parallel, nimrod/g-enabled volcanic simulation in the grid and the cloud. In e-Science (e-Science), 2010 IEEE Sixth International Conference on, Dec 2010. pages 129–136.

Paniagua S. and Soto G.. Reconocimiento de los riesgos volcánicos potenciales de la cordillera central de costa rica, américa central. Ciencia y Tecnología, 10(2).1987. Pages 49–72.

Pyle D. M. The thickness, volume and grainsize of tephra fall deposits. Bulletin of Volcanology, 51(1). 1989.1–15,.

Sáenz R., Barquero J., and Malavassi E.. Excursión al volcán irazú: Usa-cr joint seminar in vulcanology. Boletín de Vulcanología, 14. 1982. 101–116,

Scollo S., Folch A., and Costa A.. A parametric and comparative study of different tephra fallout models. Journal of Volcanology and Geothermal Research, 176(2). 2008.Pages199 – 211,

Scollo S., Prestifilippo M., Spata G., D'Agostino M., and Coltelli M.. Monitoring and forecasting etna volcanic plumes. Natural Hazards and Earth System Science, 9(5). 2009. Pages1573–1585,

Soto G. and Paniagua S.. La cordillera volcánica central (costa rica): sus peligros potenciales y prevenciones. Revista Geografía de América Central, 1992. Pages 291– 304.

Suzuki T.. The theoretical model for dispersion tephra. In Arc Volcanims: physic and tectonics, pages 94–113. Terra Scientific publishing company, Tokio, 1983.

Thomas K.. An investigation of the cervantes formation of irazú volcano, costa rica. Hanover, Dartmouth College, 1983.

Tournon J.. Magmatismes du mesozoique à l'actuel en Amerique Centrale: L'exemple de Costa Rica, des ophiolites aux andesites. PhD thesis, Paris, Université Pierre et Marie Curie., 1984.

Waldron H.. Debris Flow and Erosion control problems caused by the ash eruptions of Irazú Volcano, Costa Rica. Geological Survey Bulletin 1241, 1967.pages 1–37.

Zárate E.. Factores meteorológicos asociados a desastres causados por erup-ciones volcánicas en costa rica. Ciencia y Tecnología, 12(1–2). 1988. Páginas 41–52.